IEEE Access
Multidisciplinary | Rapid Review | Open Access Journal

Received December 28, 2017, accepted February 14, 2018, date of publication February 27, 2018, date of current version April 23, 2018.

Digital Object Identifier 10.1109/ACCESS.2018.2809797

Selective Omnidirectional Magnetic Resonant Coupling Wireless Power Transfer With Multiple-Receiver System

ZHONGYU DAI, (Student Member), ZHIJIAN FANG, (Member, IEEE), HONG HUANG, YUANJIAN HE, AND JUNHUA WANG, (Member, IEEE)
School of Electrical Engineering, Wuhan University, 430072 Wuhan, China

Corresponding author: Zhijian Fang (fangjianhust@gmail.com)

This work was supported in part by the National Natural Science Foundation of China under Project 51707138 and Project 51507114, and in part by the National Key Research and Development Plan under Project 2017YFB1201002.

ABSTRACT Magnetic resonant coupling (MRC) wireless power transfer (WPT) technology provides a novel solution to the tricky power-charging issue of densely connected sensor devices in the age of Internet of Things. Due to the cost and space constraints, the one-to-one MRC WPT is not suitable for charging the large number of sensor devices. The one-to-many MRC WPT requires less cost and space, but all receivers receive the power emitted from the transmitter disregarding the receivers' needs, which will lead to the accelerated aging even damage or malfunction of the receivers. In this paper, we propose a selective omnidirectional MRC WPT with multiple-receiver system. The power transmitted by an omnidirectional transmitter composed of three orthogonal circular coils will be received by any receiver located nearby. As the number of the transmitters reduces, the cost and space declines. Based on the band pass filter principle, the receivers selectively acquire the power at a designated frequency, which improves the energy efficiency and increase equipment service life. Moreover, for the proposed model, its magnetic field distribution of the simulation and physical experiments are carefully designed and performed, and their results are examined and analyzed in detail. They all confirm the capabilities of selective power transferring and the omnidirectional power transfer of the MRC WPT.

INDEX TERMS Magnetic resonant coupling (MRC), omnidirectional power transfer, selective power transfer, wireless power transfer (WPT).

I. INTRODUCTION

Since a 60W bulb was lighted at a 2-meter distance, based on the magnetic resonant coupling (MRC) wireless power transfer (WPT) proposed by the professor Marin Soljac̆ic' in 2007 [1], [2], the MRC WPT has been applied in various fields from daily products, medical equipment to aerospace fields [3]–[6].

Especially for the power supply of sensor devices, the MRC WPT is widely used [7]–[9]. Conventionally, the sensor devices are powered by wires or batteries [10], [11]. Complex wiring is required, and batteries must be periodically checked or replaced, which needs a great deal of human and material resources, and is not good for landscaping and environment protection. To solve these problems, the MRC WPT is applied. One mode is one-to-one MRC WPT. The receiver can receive power in long distance and owns high transmission efficiency. But one transmitter operates with only one receiver. Another mode is one-to-many MRC WPT. Many receivers just require one transmitter. But the transmission distance is shorter, and the transmitter efficiency is lower. The received power of receivers varies. Especially, the further the distance from the axis of the transmitter is, the lower received power is.

However, when sensor devices are installed in large quantities [12], [13], if the one-to-one MRC WPT or the one-to-many MRC WPT are selected to supply power, many problems will emerge. For the one-to-one MRC WPT, it requires high cost and large space because of the additional transmitters. The one-to-many MRC WPT can avoid additional transmitters when supplying power for multiple receivers. But when multiple receivers are in different locations in space, additional transmitters are still required to ensure the sufficient transmission power. To reduce the cost and the space occupation of the MRC WPT, an omnidirectional MRC

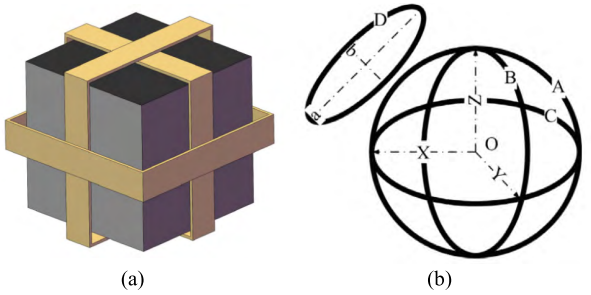

FIGURE 1. (a) Transmitter with three orthogonal square coils [14], (b) Transmitter with three orthogonal circular coils and receiver a single circular coil [15].

WPT was proposed [14]–[18]. O' Brien [14] firstly proposed the omnidirectional WPT, which comprised a transmitter with three orthogonal square coils and a receiver with three orthogonal coils as well, as shown in Fig. 1 (a). In [15], the transmitter is made up of three orthogonal circular coils and the receiver is composed by a single circular coil, as shown in Fig. 1 (b). Just one transmitter can meet the requirement that the receiver can receive power in all directions. In [17] and [18], the magnetic field distribution and the power transfer characteristics of the three orthogonal circular coils were analyzed. Based on the omnidirectional MRC WPT structure and its magnetic field distribution, a basic control method was proposed in [16] to ensure the uniform distribution of the power in all directions or to designated areas. Transmitters with three orthogonal coils in [14] and [16]–[18] require complex and high-precision control method to guarantee the uniformly distributed magnetic field in all directions, since the three orthogonal coils are controlled separately. Meanwhile, some researchers proposed a simple control method by connecting three orthogonal coils in series or parallel in [11], [19], and [20]. In this way, the magnetic field distribute in all directions, but the magnetic field distribution, the transmission distance and the efficiency in each direction are different. All control methods ensure that the receivers receive power anywhere nearby. That is, when the power is emitted from the transmitter, all the receivers receive the power regardless of their demands. It may lead to the shorter service life of sensor devices, even causes malfunctions or failures. Meanwhile, the overall energy efficiency reduces.

To solve the power supply problem of sensor devices with the omnidirectional MRC WPT, this paper proposes a selective omnidirectional MRC WPT with multiple-receiver system, which owns both omnidirectional and selective power transfer characteristics. The transmitter is composed of three orthogonal series circular coils to transmit power in all direction, while the receivers are adjusted to different resonance frequencies by matching different compensation capacitors. The transmitter is connected to a frequency-adjustable power supply through a compensation capacitor switching device. The resonant frequency of the transmitter can be adjusted to the same level of the power supply with appropriate compensation capacitor switched by the switching device. When the transmitter transmits power in all direction, only the receivers with the same frequency as the power supply and the transmitter can receive the power.

This paper is organized as follows: Section II describes the basic theoretical analysis. The coil structure of the transmitter is selected based on the theory of the MRC WPT. According to the band pass filter theory, the characteristics of the MRC WPT and the theory of the selective power transfer, the magnetic field distribution is expounded. Section III presents the design of the proposed transmitter and the receivers. Section IV shows the simulation model and the omnidirectional magnetic field distribution. Section V discusses results. Finally, conclusions are drawn in Section VI.

II. OPERATION PRINCIPLE OF OMNIDIRECTIONAL AND SELECTIVE

A. OMNIDIRECTIONAL POWER TRANSFER

In a MCR WPT, the coupling coefficient k and the quality factor Q both have inverse relationships with power loss, which means that both the coupling coefficient k and the quality factor Q have positive correlations with the system transmission efficiency [21], [22]. Therefore, for a two-coil MCR WPT, it can be obtained

$$\eta \propto k\sqrt{Q_1 Q_2} = \frac{\omega}{\sqrt{R_1 R_2}} M \tag{1}$$

For a MCR WPT with a certain resonant frequency, the transmission efficiency is only related to the mutual inductance M, based on equation (1).

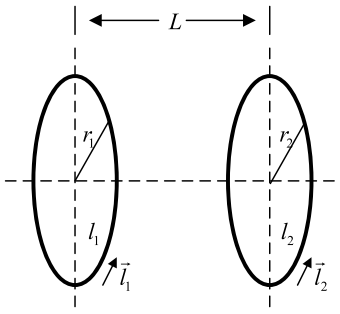

FIGURE 2. The two-coil structure MRC WPT.

In Fig. 2, according to Neumann formula, the mutual inductance of the two coils is

$$M_{12} = M_{21} = \frac{\mu_0}{4\pi} \oint_{l_1} \oint_{l_2} \frac{d\vec{l}_1 \cdot d\vec{l}_2}{L} \tag{2}$$

If the transmission efficiency remains the same and the transmission distance increases, the coil radius requires to be increased, which can be concluded from equation (1) and (2). There are two omnidirectional coil structures. One is composed of three orthogonal coils and shown in Fig. 3 (a), while the other one, as shown in Fig. 3 (b), is surrounded by many small coils to form a football-shaped sphere. Obviously, the coil radius shown in Fig. 3 (a) is larger than that

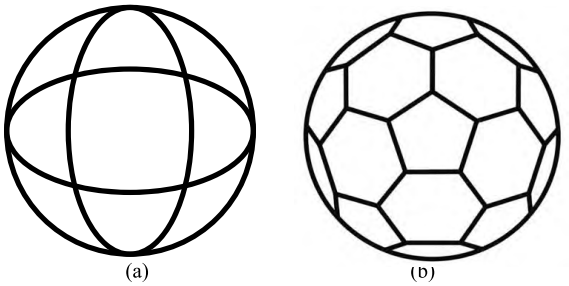

FIGURE 3. (a) The three-coil orthorhombic structure; (b) The multi-coil football-shaped structure.

shown in Fig. 3 (b). The coil structure in Fig. 3 (a) has farther transmission distance under the same transmission efficiency. Therefore, the three-orthogonal-coils structure is a better choice for the omnidirectional transmitter.

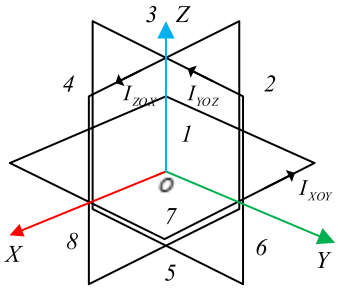

FIGURE 4. The simplified three orthogonal coil structure of the omnidirectional transmitter.

The omnidirectional coil structure is simplified, as shown in Fig. 4, and the XYZ coordinates is divided into 8 quadrants. Based on the characteristics of the three orthogonal coil structure and the passive magnetic field, it can be inferred that the magnetic field distribution remains the same in the first quadrant and the seventh quadrant, the second quadrant and the eighth quadrant, the third quadrant and the fifth quadrant, the fourth quadrant and the sixth quadrant, which indicates a symmetric structure. Supposing that the magnetic field of each coil is concentrated in the center, that is on the X, Y, Z axes, and the vector sum of the magnetic field of each coil is B. The center point of each quadrant is analyzed, as shown in Fig. 5.

$$\begin{cases} B_{1,7} = B\cos 0^\circ = B \\ B_{2,8} = B\cos 60^\circ = 0.5B \\ B_{3,5} = B\cos 90^\circ = 0 \\ B_{4,6} = B\cos 60^\circ = 0.5B \end{cases} \tag{3}$$

From equation (3), the magnitude of the magnetic field in the first and the seventh quadrant is the largest. While that of the second, the fourth, the sixth, the eighth quadrant are the same, which is only half of that in the first, the seventh quadrant. The magnetic field in the third, the fifth quadrant is 0. The result from equation (3) is an assumption under ideal conditions, which is not the true numerical results of the magnetic field distribution. But the result can indicates the magnetic field

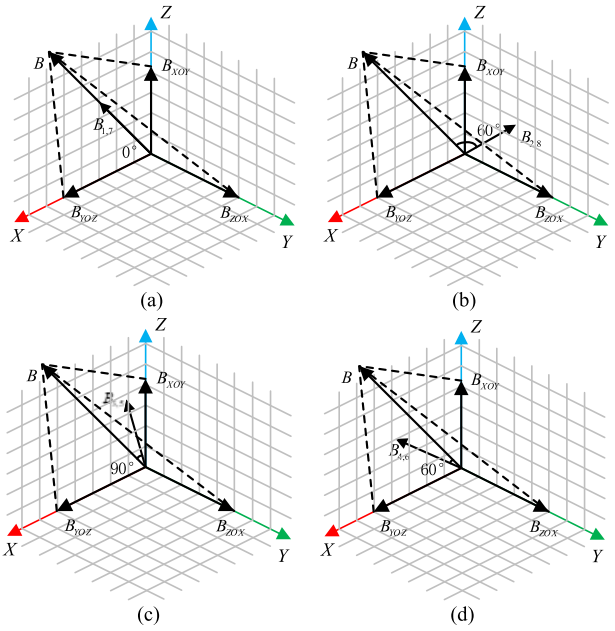

FIGURE 5. The magnetic field strength in different quadrants. (a) The first, seventh quadrant. (b) The second, eighth quadrant. (c) The third, fifth quadrant. (d) The fourth, sixth quadrant.

distribution in all quadrants. That is, the magnitude of the magnetic field distribution in the first and the seventh quadrant is the strongest, and it in the second, the fourth, the sixth and the eighth quadrant is the second, while the magnitude in the third and the fifth quadrant is the lowest. When the magnetic field is stronger, the receiver can receive more power and the transmission distance is farther. Therefore, the transmission distance is the farthest when the receiver is in the first and the seventh quadrant, the second in the second, fourth, sixth, eighth quadrant, and the nearest in the third and fifth quadrant.

B. SELECTIVE POWER TRANSFER

As shown in Fig. 6 (a), if all receivers and the transmitter are adjusted to the same resonant frequency by matching different compensation capacitors, we have

$$\begin{aligned} f_0 &= \frac{1}{2\pi\sqrt{L_{TX}C_t}} = \frac{1}{2\pi\sqrt{L_{RX1}C_{r1}}} \\ &= \frac{1}{2\pi\sqrt{L_{RX2}C_{r2}}} = \cdots = \frac{1}{2\pi\sqrt{L_{RXn}C_{rn}}} \end{aligned} \tag{4}$$

All receivers will receive the power transmitted by the transmitter, due to the same resonant frequency. In fact, since only some receivers demand power, keeping all receivers operate will waste power, or cause incorrect power supplement and damages.

When receivers are adjusted to the different resonant frequencies through the compensation capacitors, the resonant frequencies of the transmitter are also adjusted to the corresponding values by different compensation capacitors.

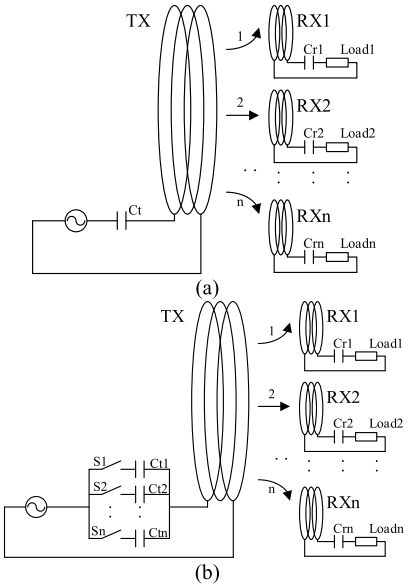

FIGURE 6. (a) MRC WPT with multiple receivers at the same resonant frequency; (b) MRC WPT with multiple receivers at different resonant frequencies.

As shown in Fig. 6 (b), it can be obtained that

$$\begin{cases} f_1 = \dfrac{1}{2\pi\sqrt{L_{TX}C_{t1}}} = \dfrac{1}{2\pi\sqrt{L_{RX1}C_{r1}}} \\ f_2 = \dfrac{1}{2\pi\sqrt{L_{TX}C_{t2}}} = \dfrac{1}{2\pi\sqrt{L_{RX2}C_{r2}}} \\ \vdots \\ f_n = \dfrac{1}{2\pi\sqrt{L_{TX}C_{tn}}} = \dfrac{1}{2\pi\sqrt{L_{RXn}C_{rn}}} \end{cases} \tag{5}$$

From equation (5), it can be found that each receiver has different resonant frequency, and the transmitter can be adjusted to the same resonant frequency of the receiver by switching to corresponding compensation capacitor. Each receiver will receive the power when it is transmitted with the corresponding frequency anywhere, which means that this MRC WPT meets the requirements of omnidirectional power transfer.

Based on the band pass filter theory and the characteristics of MRC WPT, equation (4) is modeled with the same frequency f_0 that forms passband at a same center frequency as shown in Fig. 7 (a) [23], [24]. Based on equation (5), the resonant frequency of each receiver is different from each other. The MRC WPT system can be established with distinct resonant frequencies for receivers that form passbands at separate center frequencies as shown in Fig. 7 (b) [25].

When several receivers demand the power simultaneously, the resonance frequencies of these receivers just need to be adjusted to a same value by switching the compensating capacitors. These receivers with the same frequency can receive the power at the same time. Therefore, by selecting the responding power frequency and compensation capacitor for the transmitter, only one or several power links are activated at a time. In other words, among multiple receivers, only one or several receivers are powered at the same time.

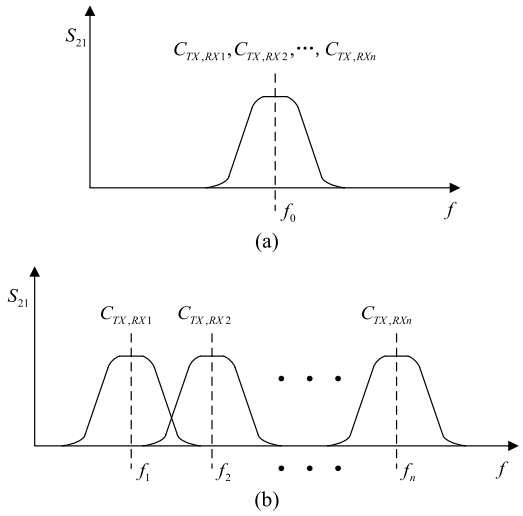

FIGURE 7. (a) Multiple receivers with a same resonant frequency [23], [24]; (b) Multiple receivers with different resonant frequencies [25].

III. PARAMETER DESIGN

A. THE TRANSMITTER

The omnidirectional transmitter is made up of three orthogonal circular coils, whose parameters are shown in table 1.

TABLE 1. The parameters of the transmitting coil.

Parameter	Value
shape	helix
material	enameled wire
wire diameter	1mm
wire spacing	1.1mm
turn	10
layer	single
coil diameter	100mm

The three orthogonal coils of omnidirectional transmitter can be connected in series or parallel. Only an excitation power supply is demanded for the series structure [10], [15], [16], while parallel structure is excited by either a single power supply or multiple power supplies [11], [14]. The control method is simple when using one power supply in the circuit, but the magnetic field distribution of the transmitter is not uniform in each direction. The power supply structure and the control method are relatively complex when several power supplies are used in the circuit, while the magnetic field can be uniformly distributed in all directions. The distribution of the sensor devices is usually non-uniform, and most sensor equipment are distributed in fixed positions. It is applicable that the region filled with a strong magnetic field of the omnidirectional transmitter is directed towards the receivers that require to be powered. Therefore, the three orthogonal circular coils are series connected. Compared with the omnidirectional MRC WPT with uniform magnetic field distribution, this model has many advantages, such as farther transmission distance, higher efficiency and easier operation

FIGURE 8. The omnidirectional transmitter.

in some directions. The physical model of the transmitter is shown in Fig. 8.

If the transmitter can be adjusted to different frequencies, it should be connected to a variable compensating capacitor. Therefore, a compensating capacitor switching device is designed to connect the omnidirectional transmitter and the power supply to switch compensation capacitors.

TABLE 2. The parameters of the receiving coil.

Parameter	Value
shape	spiral
material	enameled wire
wire diameter	0.5mm
wire spacing	0.6mm
turn	23
layer	5
coil inner diameter	3mm

B. THE RECEIVER

All receivers have the same coil structure. Different resonant frequencies are adjusted by different compensation capacitors. The parameters of the receiver are shown in table. 2.

To meet the requirements of the selective omnidirectional MRC WPT, the resonance frequency of each receiver should be adjusted to be differentiated by matching different compensating capacitors. By the measurement of a vector analyzer, the inductance of the omnidirectional transmitter $L_{TX} = 61.5\mu H$, and the receiver $L_{RX} = 30.7\mu H$, and $L_{TX} \approx 2L_{RX}$. To simplify the matching process, the monolithic capacitor is used as the compensating capacitor with withstand voltage of $1kV$ and the capacitance of $10nF$. By series-parallel connection, the receiver is matched with two sets of compensation capacitors, each set has 3 receivers, as shown in table 3.

Therefore, the two sets of frequencies the transmitter and receivers are $f_1 = 290kHz, f_2 = 640kHz$.

IV. SIMULATION OF OMNIDIRECTIONAL MAGNETIC FIELD DISTRIBUTION

According to the design of the transmitter, the corresponding simulation model is established, as shown in Fig. 9. Fig. 10 demonstrates the magnetic field distribution of the omnidirectional transmitter in different planes.

TABLE 3. The resonant frequency matching parameters.

	TX	RX
Inductance	61.5 μH	30.7 μH
the compensation capacitor C_1 under f_1	5 nF	10 nF
frequency f_1	287.01 kHz	287.24 kHz
the compensation capacitor C_2 under f_2	1 nF	2 nF
frequency f_2	641.77 kHz	642.3 kHz

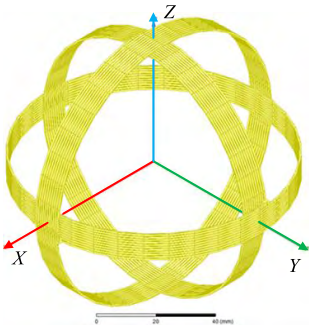

FIGURE 9. The model of the omnidirectional transmitting coil.

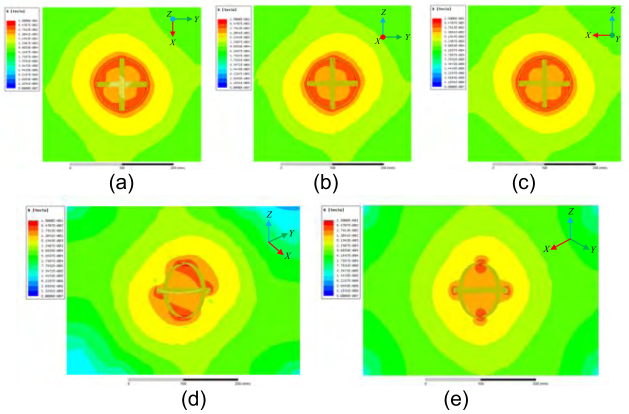

FIGURE 10. The magnetic field distribution.

Fig.10 (a), (b) and (c) are the simulation results in XOY, YOZ and ZOX planes, respectively. Fig.10 (d) is obtained in a plane where its normal vector is at a 135-degree angle to the positive axis of x and a 45-degree angle to the positive axis of y and Fig.10 (e) is obtained in a plane where its normal vector is at a 45-degree angle to the positive axis of x and y.

It can be inferred that the magnetic field distributions of omnidirectional transmitter are the almost the same in XOY, YOZ and ZOX planes, due to the symmetry. The magnetic field decreases as the distance to the transmitter increases. Because the magnetic field distribution of each coil is orthogonal since the coils are orthogonal to each other. The magnetic field distribution in the three planes of the XOY, YOZ and ZOX is generated just by the coil currents in the corresponding plane. In Fig.10 (d), the magnetic field distribution on the lower left and upper right are significantly higher than that on

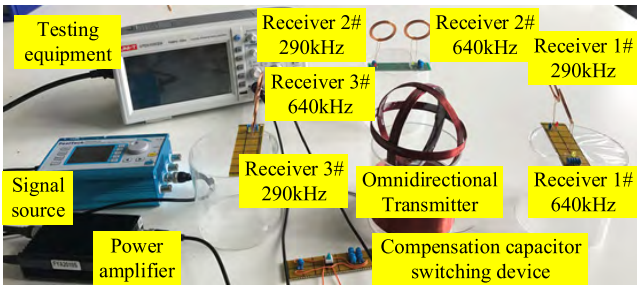

FIGURE 11. The test platform.

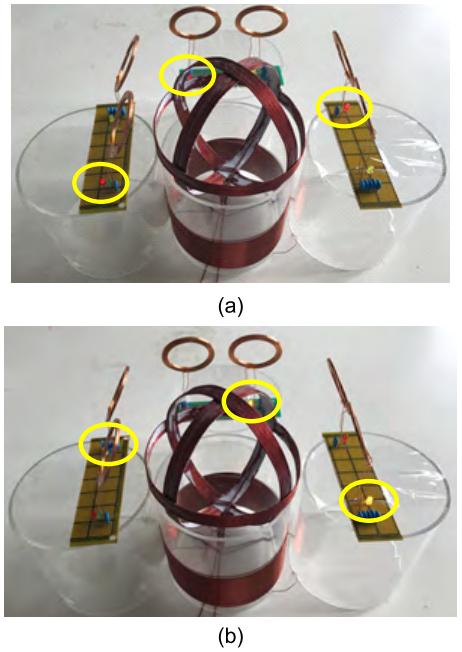

FIGURE 12. The receiver receive power selectively. (a) $f_1 = 290kHz$. (b) $f_2 = 640kHz$.

the upper left and the lower right. In Fig.10 (e), the magnetic field distribution keeps the same all around the omnidirectional transmitter. That is, the magnetic field distribution in the first and the seventh quadrant is the strongest; that in the second, the fourth, the sixth and the eighth quadrant is the second; while the magnetic field distribution in the third and the fifth quadrant is the lowest, which is consistent with the theoretical results of the equation (3) and Fig. 5.

V. EXPERIMENTS

Fig. 11 shows the corresponding test platform based on the designed omnidirectional transmitter, the compensating capacitor switching device and the receivers, etc.

The output frequencies of the power supply in Fig.12 are $f_1 = 290kHz$ and $f_2 = 640kHz$. The LED will be lighted when receiver receives power. When the frequency $f_1 = 290kHz$, the red LEDs attached to three receivers are bright as shown in Fig.12 (a), and the other three green LEDs attached to receivers frequency $f_2 = 640kHz$.

Furthermore, the voltage waveforms and amplitudes of the transmitter and receivers are shown in Fig. 13 (a) and (b). The

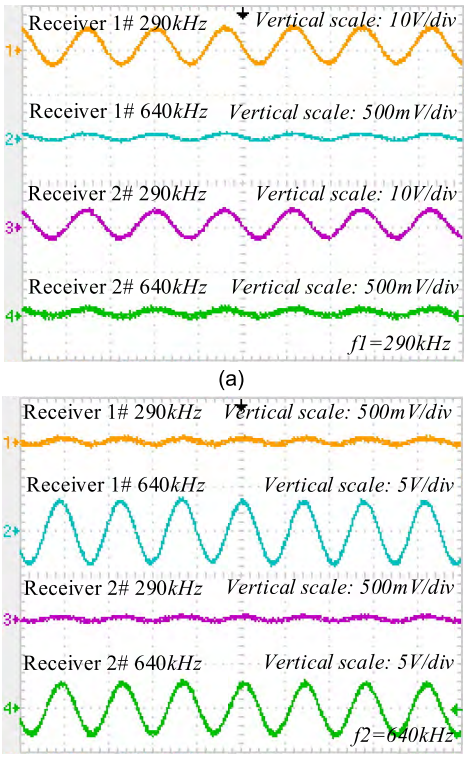

FIGURE 13. The waveforms of different receivers. (a) $f_1 = 290kHz$. (b) $f_2 = 640kHz$.

voltage amplitude of receiver 1# 290kHz is higher than the receiver 2# 290kHz, while receiver 1# 640kHz and receiver 2# 640kHz barely receive power at frequency $f_1 = 290kHz$. When the frequency is adjusted to $f_2 = 640kHz$, only the receiver 1# 640kHz and receiver 2# 640kHz can receive the power, and the voltage amplitudes are about 8V and 7V respectively. It verify that the MRC WPT with multiple-receiver system has the function that only the receiver requiring power receive the power in all directions.

When the distances between the receivers and the center of the transmitter are $L_1 = 18.5cm$, $L_2 = 17cm$, $L_3 = 12cm$, the receivers' voltage amplitudes are around 3.7V, as shown in Fig. 14(a), in the quadrant 1, 2 and 3, respectively. The waveforms of the transmitter and the receivers are shown in Fig. 14(b). The Ch1, Ch2, Ch3 channel measure the receivers' voltage waveforms, and the Ch4 channel use a high voltage probe with an attenuation rate of 100:1 to measure the voltage waveform of the transmitter.

When the distances between the transmitter center and each receiver all are $L = 12cm$ as shown in Fig. 15(a), the voltage waveforms of the three receivers are shown in Fig. 15(b), and the voltage amplitudes of the receivers are $V_1 = 12.3V$, $V_2 = 7.9V$, $V_3 = 3.7V$, respectively.

From the experimental results shown above, when the distances from different receivers to the transmitter center is $L_1 > L_2 > L_3$, the receivers' voltages are the same and the voltage amplitude of receivers is $V_1 > V_2 > V_3$. The voltage amplitude and the transmission distance are both

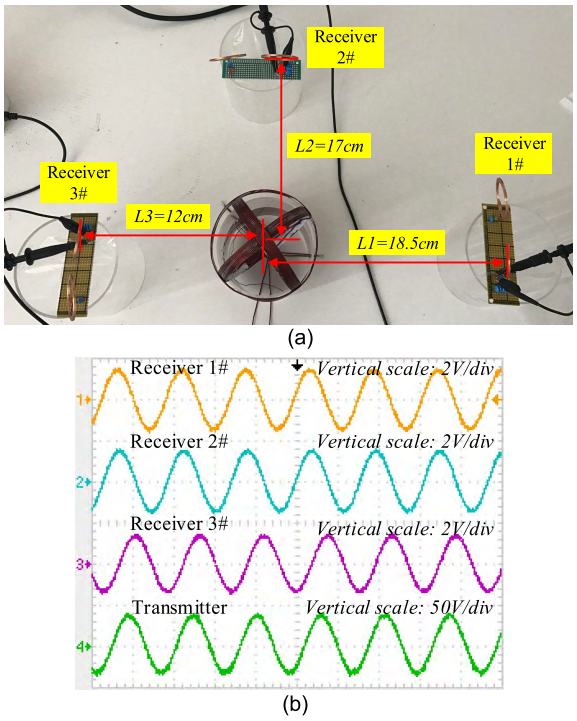

FIGURE 14. Scenario I. (a) Receivers receive the same power. (b) The waveforms of the transmitter and the receivers.

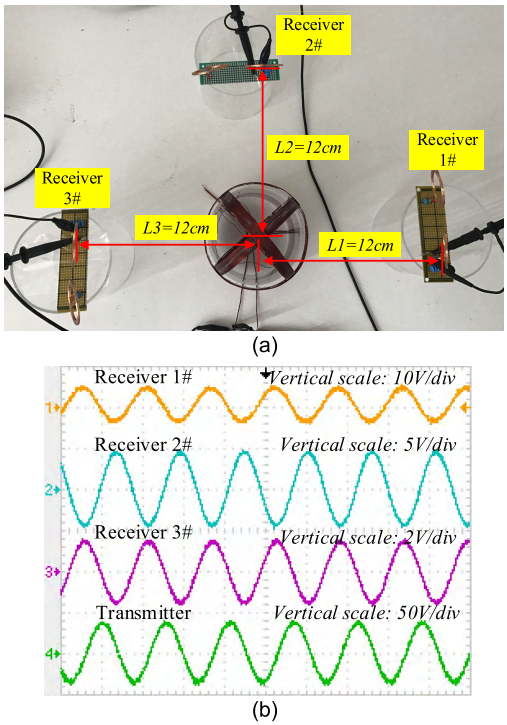

FIGURE 15. Scenario II. (a) The distances are the same. (b) The waveforms of the transmitter and the receivers.

positively correlated with the magnetic field. Consequently, the magnitude of the magnetic field $|B_1|$ is the strongest in the first quadrant, $|B_2|$ in the second quadrant is the second strongest, while $|B_3|$ in the third quadrant is the weakest. The magnetic field distribution is quadrant-symmetric deduced

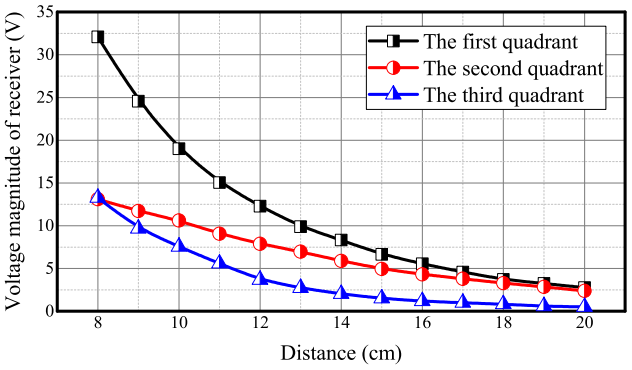

FIGURE 16. The voltage amplitude of the receiver against the distance between the receiver and the transmitter.

from the structure characteristic of the omnidirectional transmitter. It can be obvious that $|B_{1,7}| > |B_{2,4,6,8}| > |B_{3,5}|$. In addition, all magnetic induction lines form closed loops based on the magnetic field is a passive field. The magnetic field distribution is close to the state of uniform distribution, rather than a big difference.

When the distance between the receivers and the center of the transmitter varies, the voltage amplitude of the receiver in the different quadrant is tested, as shown in Fig. 16.The trend of the changes in the voltage amplitude of the receiver and the distance between the receiver and the transmitter are shown. The voltage amplitude decreases as the distance increases. The decreasing rate of the voltage amplitude is the fastest in the first quadrant, while the slowest in the third quadrant. In the range of 8cm to 20cm, the voltage amplitude of the first quadrant is always higher than that of the second quadrant, and that of the third quadrant is the lowest. When the distance is 8cm, the voltage amplitude of the first quadrant is 32.1V and is the highest, which is twice times more than the second and third quadrant whose voltage amplitudes are 13.2V. The voltage amplitudes of the first quadrant and the second quadrant are almost same, about 2.5V, while that of the third quadrant is only 0.51V, in a distance of 20cm. The trends of the voltage amplitude of each quadrant shown in Fig. 16 provides a reference for the installation of the receiver position of the selective omnidirectional MRC WPT with multiple-receiver system.

VI. CONCLUSION

In this paper, based on the theory of the MRC WPT characteristics and the band pass filter principle, a selective omnidirectional MRC WPT with multiple-receiver system is proposed. Omnidirectional MRC WPT can transfer power in all directions according to the omnidirectional transmitter, and only the receiver need power can receive it based on the selective MRC WPT, which will improve the service life of the devices powered from the receivers and the energy efficiency. The design and demonstration in this paper provide a guideline for the power supply problem of densely connected sensors in the age of IoT.

REFERENCES

[1] A. Karalis, J. D. Joannopoulos, and M. Soljačić, "Efficient wireless *non-radiative mid-range* energy transfer," *Ann. Phys.*, vol. 323, no. 1, pp. 34–48, 2008.
[2] A. Kurs, A. Karalis, R. Moffatt, J. D. Joannopoulos, P. Fisher, and M. Soljačić, "Wireless power transfer via strongly coupled magnetic resonances," *Science*, vol. 317, no. 5834, pp. 83–86, 2007.
[3] C. Zhang and Y. Chen, "Wireless power transfer strategies for cooperative relay system to maximize information throughput," *IEEE Access*, vol. 5, pp. 2573–2582, 2017.
[4] M. R. Basar, M. Y. Ahmadm, J. Cho, and F. Ibrahim, "Stable and high-efficiency wireless power transfer system for robotic capsule using a modified helmholtz coil," *IEEE Trans. Ind. Electron.*, vol. 64, no. 2, pp. 1113–1122, Feb. 2017.
[5] P. S. Yedavalli, T. Riihonen, X. Wang, and J. M. Rabaey, "Far-field RF wireless power transfer with blind adaptive beamforming for Internet of Things devices," *IEEE Access*, vol. 5, pp. 1743–1752, 2017.
[6] G. Monti *et al.*, "Wireless power transfer with three-ports networks: Optimal analytical solutions," *IEEE Trans. Circuits Syst. I, Reg. Papers*, vol. 64, no. 2, pp. 494–503, Feb. 2017.
[7] T. Liu, X. Wang, and L. Zheng, "A cooperative SWIPT scheme for wirelessly powered sensor networks," *IEEE Trans. Commun.*, vol. 65, no. 6, pp. 2740–2752, Jun. 2017.
[8] V. V. Mai, W.-Y. Shin, and K. Ishibashi, "Wireless power transfer for distributed estimation in sensor networks," *IEEE J. Sel. Topics Signal Process.*, vol. 11, no. 3, pp. 549–562, Apr. 2017.
[9] R. Shea *et al.*, "Location-based augmented reality with pervasive smartphone sensors: Inside and beyond Pokemon Go!" *IEEE Access*, vol. 5, pp. 9619–9631, 2017.
[10] Y. Yang *et al.*, "Stability enhanced, repeatability improved Parylene-C passivated on QCM sensor for aPTT measurement," *Biosensors Bioelectron.* vol. 98, pp. 41–46, Dec. 2017.
[11] N.-C. Kuo, B. Zhao, and A. M. Niknejad, "Bifurcation analysis in weakly-coupled inductive power transfer systems," *IEEE Trans. Circuits Syst. I, Reg. Papers*, vol. 63, no. 5, pp. 727–738, May 2016.
[12] M. Guan, K. Wang, D. Xu, and W.-H. Liao, "Design and experimental investigation of a low-voltage thermoelectric energy harvesting system for wireless sensor nodes," *Energy Convers. Manage.*, vol. 138, pp. 30–37, Apr. 2017.
[13] C. M. Caffrey, T. Sillanpää, H. Huovila, J. Nikunen. S. Hakulinen, and P. Pursula, "Energy autonomous wireless valve leakage monitoring system with acoustic emission sensor," *IEEE Trans. Circuits Syst. I, Reg. Papers*, vol. 64, no. 11, pp. 2884–2893, Nov. 2017.
[14] K. O'Brien, *Inductively Coupled Radio Frequency Power Transmission System for Wireless Systems and Devices*. Herzogenrath, Germany: Shaker Verlag Gmbh, 2007.
[15] D. Wang, Y. Zhu, H. Guo, X. Zhu, T. Mo, and Q. Huang, "Enabling multi-angle wireless power transmission via magnetic resonant coupling," in *Proc. IEEE Int. Conf. Comput. Converg. Technol.*, Dec. 2012, pp. 1395–1400.
[16] C. Zhang, D. Lin, and S. Y. Hui, "Basic control principles of omnidirectional wireless power transfer," *IEEE Trans. Power Electron.*, vol. 31, no. 7, pp. 5215–5227, Jul. 2016.
[17] D. Lin, C. Zhang, and S. Y. R. Hui, "Mathematical analysis of omnidirectional wireless power transfer—Part-I: Two-dimensional systems," *IEEE Trans. Power Electron.*, vol. 32, no. 1, pp. 625–633, Jan. 2016.
[18] D. Lin, C. Zhang, and S. Y. R. Hui, "Mathematic analysis of omnidirectional wireless power transfer—Part-II: Three-dimensional systems," *IEEE Trans. Power Electron.*, vol. 32, no. 1, pp. 613–624, Jan. 2017.
[19] Z. Ouyang, Z. Zhang, M. A. E. Andersen, and O. C. Thomsen, "Four quadrants integrated transformers for dual-input isolated DC–DC converters," *IEEE Trans. Power Electron.*, vol. 27, no. 6, pp. 2697–2702, Jun. 2012.
[20] O. Jonah, S. V. Georgakopoulos, and M. M. Tentzeris, "Orientation insensitive power transfer by magnetic resonance for mobile devices," in *Proc. IEEE Wireless Power Transf.*, May 2013, pp. 5–8.
[21] E. I. Green, "The story of Q," *Amer. Sci.*, vol. 43, no. 4, pp. 584–594, 1955.
[22] J. O. Mur-Miranda *et al.*, "Wireless power transfer using weakly coupled magnetostatic resonators," in *Proc. Energy Convers. Congr. Expo.*, Sep. 2010, pp. 4179–4186.
[23] I. Awai and T. Ishizaki, "Superiority of BPF theory for design of coupled resonator WPT systems," in *Proc. Asia–Pacific Microw. Conf.*, Dec. 2012, pp. 1889–1892.
[24] D. Ha, T.-C. Lee, D. J. Webery, and W. J. Chappell, "Power distribution to multiple implanted sensor devices using a multiport bandpass filter (BPF) approach," in *IEEE MTT-S Int. Microw. Symp. Dig.*, Jun. 2014, pp. 1–4.
[25] Y.-J. Kim, D. Ha, W. J. Chappell, and P. P. Irazoqui, "Selective wireless power transfer for smart power distribution in a miniature-sized multiple-receiver system," *IEEE Trans. Ind. Electron.*, vol. 63, no. 3, pp. 1853–1862, Mar. 2016.

ZHONGYU DAI received the B.Sc. degree from Wuhan University in 2014, where he is currently pursuing the Ph.D. degree. His main research interests include wireless transmission technology based on magnetic resonance, applied electromagnetics, and system equipment for power transmission and distribution.

ZHIJIAN FANG received the B.S. and Ph.D. degrees in electrical engineering and automation from the Huazhong University of Science and Technology, Wuhan, China, in 2010 and 2015, respectively. Since 2015, he has been a Post-Doctoral Research Fellow with the School of Electrical Engineering, Wuhan University, Wuhan. From 2016 to 2017, he was a Post-Doctoral Research Fellow with the Department of Electrical and Computer Engineering, Ryerson University, Toronto, ON, Canada. His research interests include high performance dc/dc converter, battery charger, and renewable energy applications.

HONG HUANG received the B.Sc. degree from Dongbei University in 2017. She is currently pursuing the master's degree with Wuhan University. Her main research interests include wireless transmission technology based on magnetic resonance and applied electromagnetics.

YUANJIAN HE received the bachelor's degree from North China Electric Power University in 2015. He is currently pursuing the M.E.E. degree with Wuhan University. His main research interest covers the wireless transmission technology based on magnetic resonance, power electronics, and applied electromagnetics.

JUNHUA WANG was born in Linyi, Shandong, China, in 1981. He received the Ph.D. degree from The Hong Kong Polytechnic University, Hong Kong, China, in 2012. In 2012, he joined Carnegie Mellon University as a Post-Doctoral Researcher and then as a Research Fellow, GATE Center for Electric Drive Transportation, MI, USA. He is currently a Professor with the School of Electrical Engineering, Wuhan University. His main research interests include wireless transmission technology based on magnetic resonance, applied electromagnetics, system equipment for power transmission and distribution.